Journal of Polymer Research (2022) 29:506
https://doi.org/10.1007/s10965-022-03357-z

ORIGINAL PAPER

Formation of craze-like pattern in polypropylene UV-induced surface cracking

Amanda de S. M. de Freitas[1,2] · Jéssica S. Rodrigues[2] · Vagner R. Botaro[2] · Ana Paula Lemes[1] · Sandra Andrea Cruz[3] · Walter R. Waldman[2]

Received: 28 June 2022 / Accepted: 7 November 2022 / Published online: 12 November 2022

Abstract
Polypropylene (PP) samples were exposed to accelerated aging with UV-C light and showed a morphology inside the crackings like that of thermoplastic polymers under stress, known as craze. Herein we used the well-established photodegradation of polypropylene to build the relationship between the phenomenon of fibrillation inside the crackings and the microvoid formation during the evolution of the craze process. The basis of our proposition is the similarity of the processes but the stress source: whereas an external tensile stress load drives the craze, in photodegradation the stress comes from the changes caused by the crystallization, which reduces volume, creating tensions and forming cracks. We followed the polypropylene photodegradation using Scanning Electron Microscopy (SEM), tensile tests, Dynamic Mechanical Thermal Analysis (DMTA), Fourier Transform Infrared Spectroscopy (FTIR), and X-ray Diffractometry (XRD) to prove the correlation between the cracking evolution and the craze mechanism. From this similarity, we paved the way to applying the current knowledge about the craze phenomenon to understand better the cracking evolution on polypropylene surfaces.

Keywords Photodegradation of polypropylene · Craze morphology · Crack formation mechanism · Surface changes in polypropylene

Introduction

When exposed to ultraviolet light, polymeric materials such as polypropylene, are prone to chemical modification known as photodegradation [1, 2]. The interaction of the polymer with light occurs initially in the so-called chromophore groups, which harvest the light and transfer its energy to foster homolytic scission and the formation of the free radicals, leading to the auto-oxidation cycle [3]. Although PP has no intrinsic chromophore groups in its regular structure, these can be generated through defects during the polymerization process, the presence of impurities and/or additives. Thus, the generated chromophore groups can capture the energy of UV light to initiate the reactions of the autoxidation cycle [4, 5].The photodegradation process leads to changes in the surface of the material [6] that can propagate through the bulk of the polymer as the degradation progresses [3, 7]. Some works in the literature studied polymeric photodegradation [8–11], and presented cracks formation as the main phenomenon associated with the decrease in mechanical properties, such as the increase in fragility observed in photodegraded polymers [12]. Although cracks formation is responsible for material weakening, it is essential to emphasize that it begins with the development of microvoids, which evolve into a fibrillation process, and further rupture of fibrils forming a crack [13].

On the other hand, the craze phenomenon (Fig. 1) occurs in thermoplastic polymers when a tensile load deforms a region of the polymeric material. Plastic deformation (Fig. 1A) is caused by stresses that exceed the elastic limit of the material [14]. This whole process that precedes the fracture of the material occurs when the stress

Amanda de S. M. de Freitas and Jéssica S. Rodrigues are contributed equally to this work.

✉ Walter R. Waldman
walter.waldman@gmail.com

[1] Federal University of São Paulo - UNIFESP, São José Do Campos, SP, Brazil

[2] Federal University of São Carlos - UFSCar, Sorocaba, SP, Brazil

[3] Federal University of São Carlos - UFSCar, São Carlos, SP, Brazil

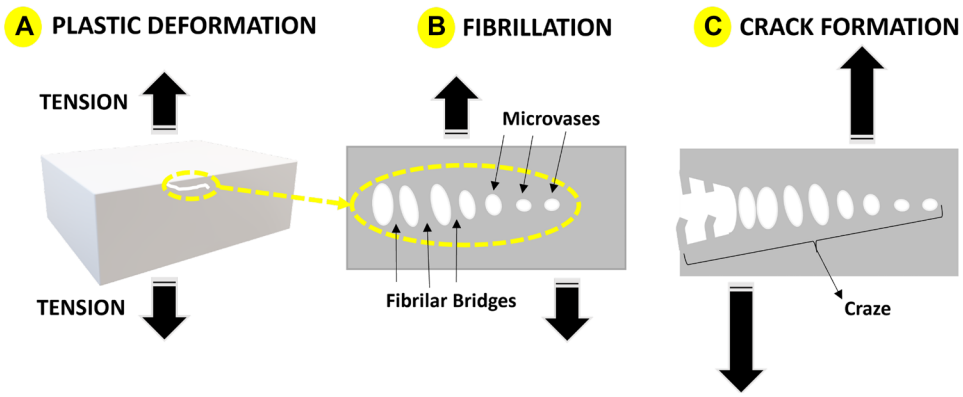

Fig. 1 Schematic representation of the traditional craze process: **A** Plastic deformation caused by stresses in a region in the polymeric material; **B** Emergence of small microvoids and fibrillar bridges in a plane perpendicular to the applied tension; **C** Fibrils extend and narrow, leading to the growth and rupture of microvoids, which form the cracks

applied to the part is greater than the tensile strength of this polymer [15].

This deformation creates microvoids in a plane perpendicular to the elongation direction. To Stabilize the voids, fibrils promote connections between the cracking walls [16], acting as fibrillar bridges by structuring the cracks, and enabling the material to withstand a high level of stress (Fig. 1B). If the tensile load applied is sufficient, these fibrils will extend and narrow to the point where they eventually break [17], leading to microvoids growth and material breakage (Fig. 1C). In this process, mechanical energy is dissipated by the flow. The localized flow of chains by fibrillation occurs due to the spacing between the cracking walls [18]. The region where these processes occur is called the "craze" [14] and gives the process its name. It is noteworthy that fibrillation is different from a standard crack which can support the load along its entire length. In terms of dimension, crazes are constituted by polymer fibrils with approximately 5–15 nm diameter, separated by elongated voids with diameters up to 50 nm [19]. On the other hand, cracks present dimensions larger than crazes.

Despite the works in the literature [20–22] studying the formation and growth of crazes, as far as we know, there is no report about their formation through PP photodegradation, as proposed in this work. Here, PP samples were exposed to UV-C light for 196 h to carry on the photodegradation process. PP samples before and after photodegradation were analyzed using scanning electron microscopy (SEM), tensile testing, dynamic mechanical thermal analysis (DMTA), Fourier transform infrared spectroscopy (FTIR) and x-ray diffractometry (XRD). SEM allowed the visualization of the interior of the cracks in the sample. A morphology similar to the craze phenomenon was revealed when we explored the interior of these cracks at higher magnifications of these regions. The literature widely reports studying the effects and morphology changes due to photodegradation in polymeric materials. However, comparison of the morphology observed in traditional craze and fibrillation due to photodegradation is still a gap in the literature on polymeric materials, which this work seeks to fill.

Experimental

Photodegradation

To prepare the samples, transparent polypropylene was used, with a thickness of 0.35 mm, cut into rectangles of 15×100 mm. The samples were exposed for 196 h to 15 W UV-C fluorescent germicidal lamps (Osram brand, model TUV15W) in an aging chamber as described by Cacuro et al. [23]. The maximum emission of the lamps was 254 nm, and the incident energy was 610 ± 10 μW.cm^{-2}. The distance between the lamps and samples was 0.2 m.

Characterization of samples

All analyses were performed on PP samples without exposure to light (0 h) and after exposure to UV-C light (196 h). Morphological analysis of the sample surface was carried out with a Quanta 650 FEG scanning electron microscope. The samples were first spray-coated with a thin gold layer using a low deposition rate. The coating of the samples was carried out in a Denton Vacuum metallizer, Desk V model, for 60 s, at a current of 30 mA and ambient pressure of 0.05 Torr. The samples were placed at the maximum distance from the target to avoid damage; a secondary electron detector and incident energy of 3 kV was used. The tensile tests were performed in a universal mechanical testing machine EMIC, DL 10,000 model, with a speed of 50 mm. min^{-1}, and a load cell of 250 N. PP samples were cut to 40/5/0.35 mm in height, width, and thickness, respectively. The distance between the test claws was 2 cm. The dynamic mechanical thermal behavior was analyzed in a DMTA model Q 800 equipment (TA Instruments) using a tensioned film clamp. The specimens had approximate dimensions of 10/7/0.35 mm in height, width, and thickness. A frequency

of 1 Hz, preload of 0.01 N, amplitude of 4000 µm, and heating rate of 5 °C.min^{-1}, from -25 to 150 °C, were applied. The chemical composition of the films was analyzed in a Nicolet Summit IR 200 spectrophotometer in ATR mode, with absorbance measurement using 126 scans and a nominal resolution of 4.0 cm^{-1} in the range of 4000 to 400 cm^{-1}. XRD analysis was performed in an XRD-7000 SHIMADZU diffractometer with a Ni filter, Cu Kα radiation, 0.6/sec step, and 2°.min^{-1} speed using a voltage and current of 40 kV and 50 mA, respectively. The visual appearance of the samples was recorded using a cell phone camera of 12 megapixels to take photos with a resolution of 4608 × 2592 pixels.

Results and discussion

Chemical and structural modifications

PP photodegradation can be followed by comparing the FTIR spectra of the samples before and after exposure to the UV-C light, using the characteristic absorption bands of hydroxyl (OH) and carbonyl (C = O), highlighted in Fig. 2A. Oxidative reactions lead to the emergence of these chemical species evidencing the oxidative degradation of polypropylene [23, 24].

The bands at 3300–3700 cm^{-1} and 1650–1850 cm^{-1} are characteristic of O–H (hydroxyl) bond stretching and C = O (carbonyl) bond elongation, respectively. These chemical groups are commonly associated with polypropylene photodegradation [3, 25, 26]. Comparing the spectra of polypropylene before and after exposure, the sample with 196 h of UV-C light exposure shows higher absorption intensity in these regions, indicating the evolution of photodegradation in the polymeric material.

X-ray diffraction results were analyzed using the Joint Committee Powder Diffraction Standards (JCPDS) database to attribute crystalline phases and structures [27]. The PP diffractogram, Fig. 2B (before photodegradation (0 h)) clearly shows the characteristic diffraction of the α crystalline form of polypropylene with the presence of peaks at 2Θ = 19.35 (040) α, 2Θ = 23.05 (117) γ, and 2Θ = 24.40 (131) α. After photodegradation (196 h), these peaks became more intense, indicating an increase in crystalline fraction as a function of degradation time, attributed to chemicrystallization [28].

The visual changes caused by photodegradation, such as yellowing and deformation of the material, are shown in Fig. 2C [23]. It is noteworthy that the deformation is caused by the decrease in the volume on the surface of the material compared to the bulk due to the crystallization produced

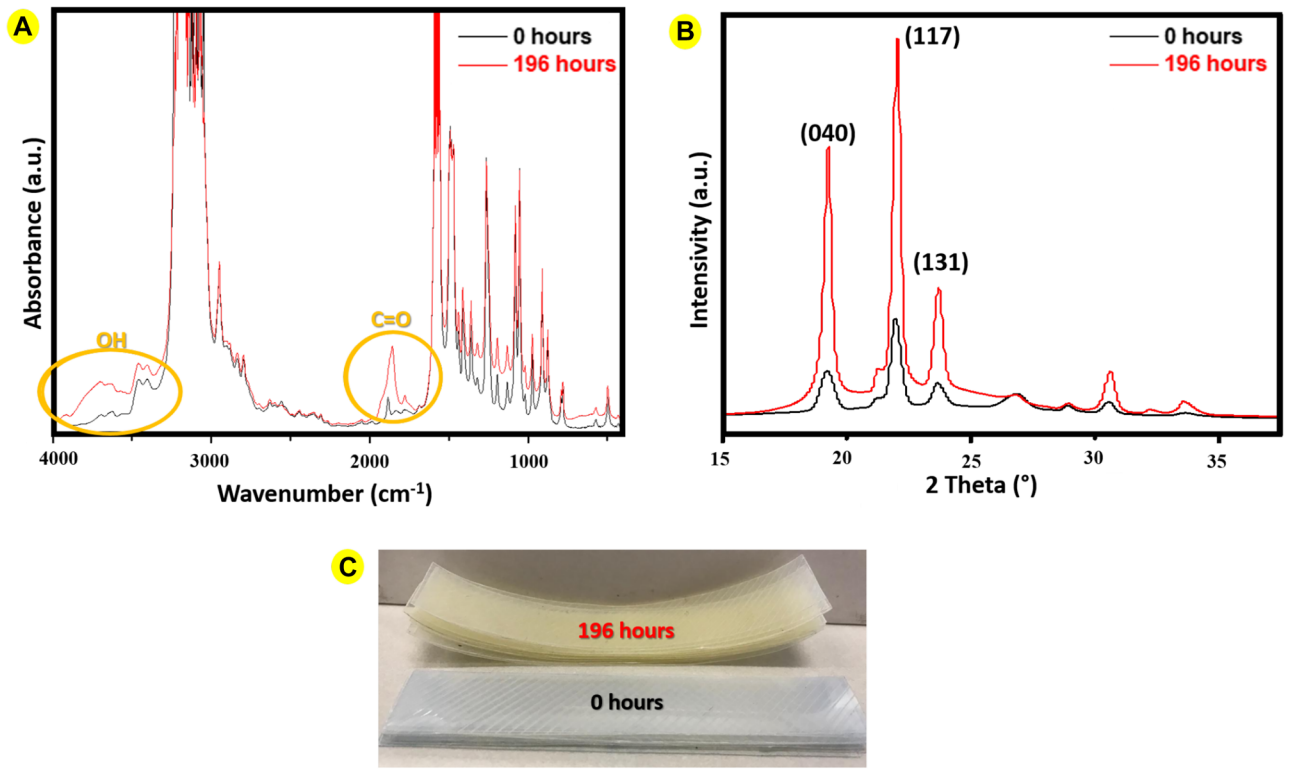

Fig. 2 Characterization results of polypropylene samples without exposure to UV-C light (0 h) and after exposure (196 h): **A** normalized FTIR spectra, **B** X-ray diffractograms, and **C** Photographic record of the samples

by the photodegradation [29, 30]. The yellowing is mainly caused by the formation of chromophore groups [31, 32] and by-products of the phenolic antioxidants action [33]. Photodegradation also leads to opacity in the samples, which evolves to yellowing with longer exposure to light [34].

Mechanical and thermal analysis

DMTA analysis, Fig. 3A–C, allowed us to characterize the materials in a temperature range from -25 to 150 °C, obtaining storage modulus (E') and loss modulus (E'') curves, Fig. 3.

DMTA analysis aims to correlate macroscopic properties, such as mechanical, with first-order and second-order thermodynamic transitions, such as the glass transition (T_g), and secondary relaxations associated with the phases crystalline and amorphous [35]. The maximum observed loss modulus (E''), in the glass transition region is due to the high conversion of mechanical energy into heat through the micro-Brownian movements of the main chain segments. Analyzing the E" curves as a function of temperature, peaks at 1.6 and 9.3 °C are observed for the control samples and the photodegraded samples, respectively. This increase in Tg (Fig. 3A) after exposure to photodegradation may be associated with an increase in crystalline phase upon immobilization of the amorphous phase. This result corroborates those obtained by XRD analysis. An additional effect observed is a broadening in E'' peak attributed to an increased presence of different microenvironments (amorphous, crystalline, and interface), resulting in a broader distribution of relaxation times [36]. The PP loss modulus before photodegradation was higher than after photodegradation, 156 MPa and 87 MPa, respectively. This result was not expected once theoretically the increase in crystallinity directly reflects the increase in E" [37], however, the observed reduction can be related to the presence of crazes/cracks generated in PP after photodegradation. Between 60–70 °C, the materials do not show significant differences in behavior for the loss modulus.

In Fig. 3B, regarding the behavior of E', all samples showed a response at a temperature of -20 °C; however, PP before photodegradation showed the highest storage value (E' = 32,222 MPa). It was also possible to verify that from 100 °C, the samples start to have the same behavior, revealing that the high crystallinity of PP after photodegradation no longer causes effects on the mechanical behavior of the materials; at this point, the composites become equal [38].

The photodegradation of polyolefins in general tends to the formation of volatiles during the process [11, 39]. However, this is not the main factor to produce mechanical stress that will generate the cracks, but the physicochemical changes, such as chain scission and the consequent reduction in molar mass, associated with the presence of cracks on the surface of the sample, contribute to embrittlement. The chemical and physical changes of polymeric materials undergoing photodegradation

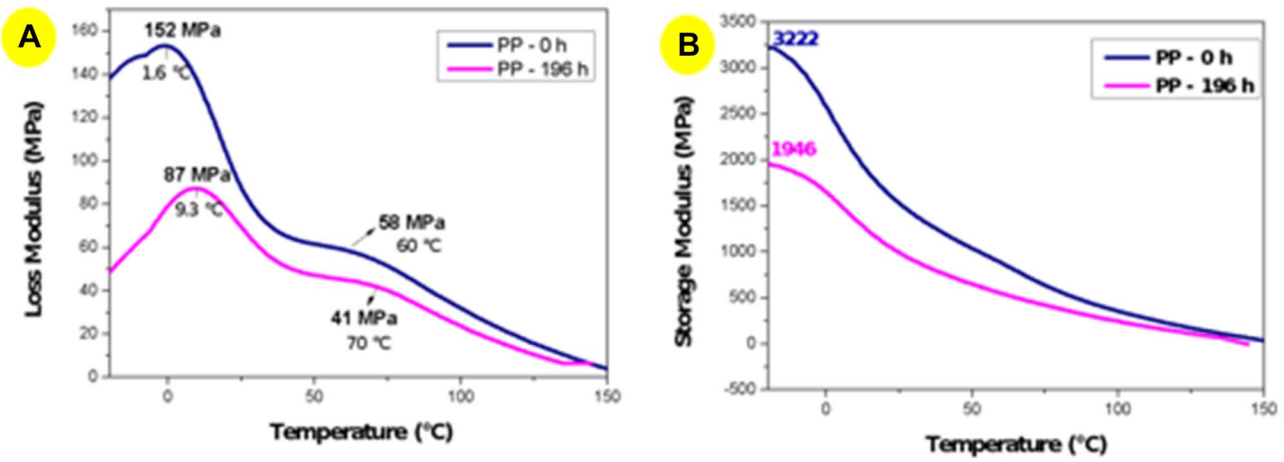

C

	Elongation at Rupture (mm/mm)	Tensile Strength (N/mm²)	Elastic Modulus (MPa)
0 h	1.033 ± 0.251	33.318 ± 1.673	818.040 ± 98.972
196 h	0,011 ± 0.004	6.944 ± 1.244	823.289 ± 69.089

Fig. 3 Dynamic mechanical thermal analysis of polypropylene samples without exposure to UV-C light (0 h) and after exposure (196 h). DMTA test results: **A** loss modulus (E'') and **B** storage modulus (E'). The tensile test results: **C** Elongation at rupture, tensile strength, and elastic modulus

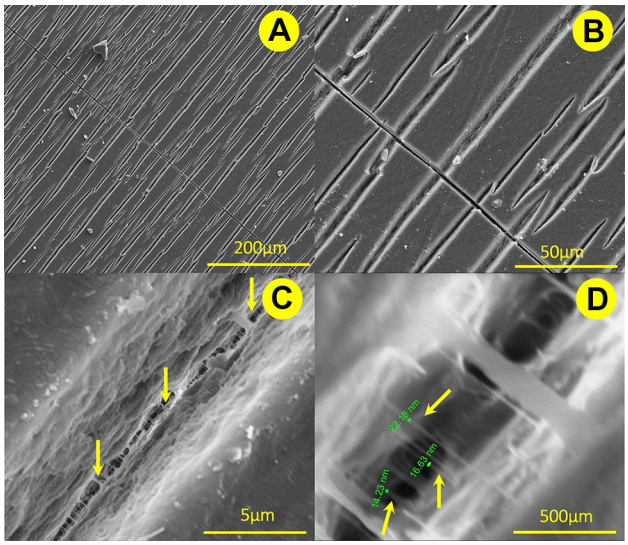

Fig. 4 Micrographs of polypropylene samples after 196 h of photodegradation. **A** The surface degradation pattern, bar size 200 µm. **B** Magnification of surface degradation pattern, bar size 50 µm. **C** Focus inside the cracks, bar size 5 µm. **D** Measurements of fibril dimensions, bar size 500 nm

affect their mechanical properties, especially elongation at break and tensile strength, two highly relevant properties in the lifetime of the material. The results (tensile strength, elongation at rupture, and elastic modulus) obtained for the tensile test are shown in Fig. 3C. In general, PP photodegradation causes a significant decrease in elongation of rupture and tensile strength compared to PP before photodegradation. These behaviors were attributed to the scission of the binding of molecules in the intra- and inter-spherulitic regions, which generate a significant presence of chromophore groups in these regions, exhibited by crystals growing during PP crystallization [40, 41]. Also, cracks may have contributed to reducing these properties, with a change from a more ductile to a more fragile behavior after photodegradation.

Morphological analyses

After 196 h of exposure to UV-C light, the samples showed visual changes, becoming opaque, yellowish and deformed. Surface analysis of PP before light exposure was performed to serve as a comparison, Fig. SI. Figure 4A, B show parallel cracks across the surface that were not present in the PP sample before exposing the samples to the UV-C light. Figure 4C, D present the magnifications inside the crack.

Fibrils inside the crackings produced after 196 h of exposure to UV-C light are shown in Fig. 4. Figure 4A, B revealed a distribution pattern of parallel cracks perpendicular to the cracking wall. These cracks have dimensions between 3.5 and 5 µm in width and length of several millimeters. The inner morphology of the fissures shows a progressive degradation of the polymer from the surface toward the polymeric bulk

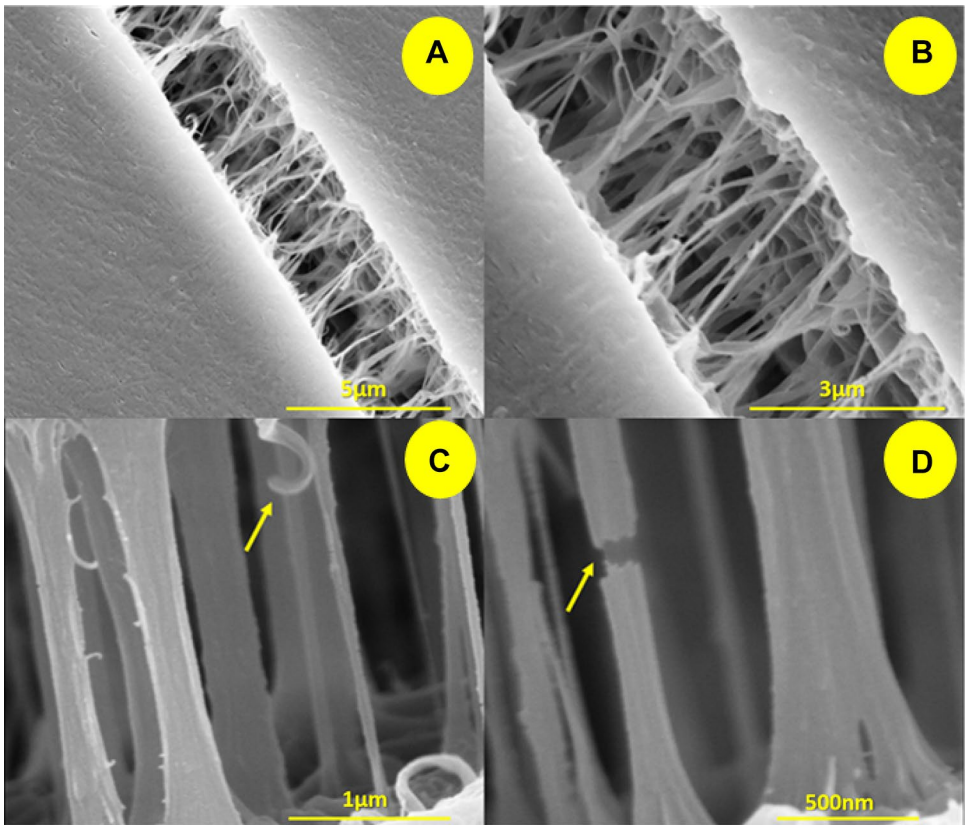

Fig. 5 Micrographs inside the cracks of the polypropylene samples after 196 h of photodegradation. **A** Inner crack region, bar size 5 µm. **B** Magnification of the inner crack region, bar size 3 µm. **C** Highlight with yellow arrows at the ends of a ruptured fibril, bar size 1 µm. **D** Highlight with yellow arrows in the fibril rupture area, bar size 500 nm

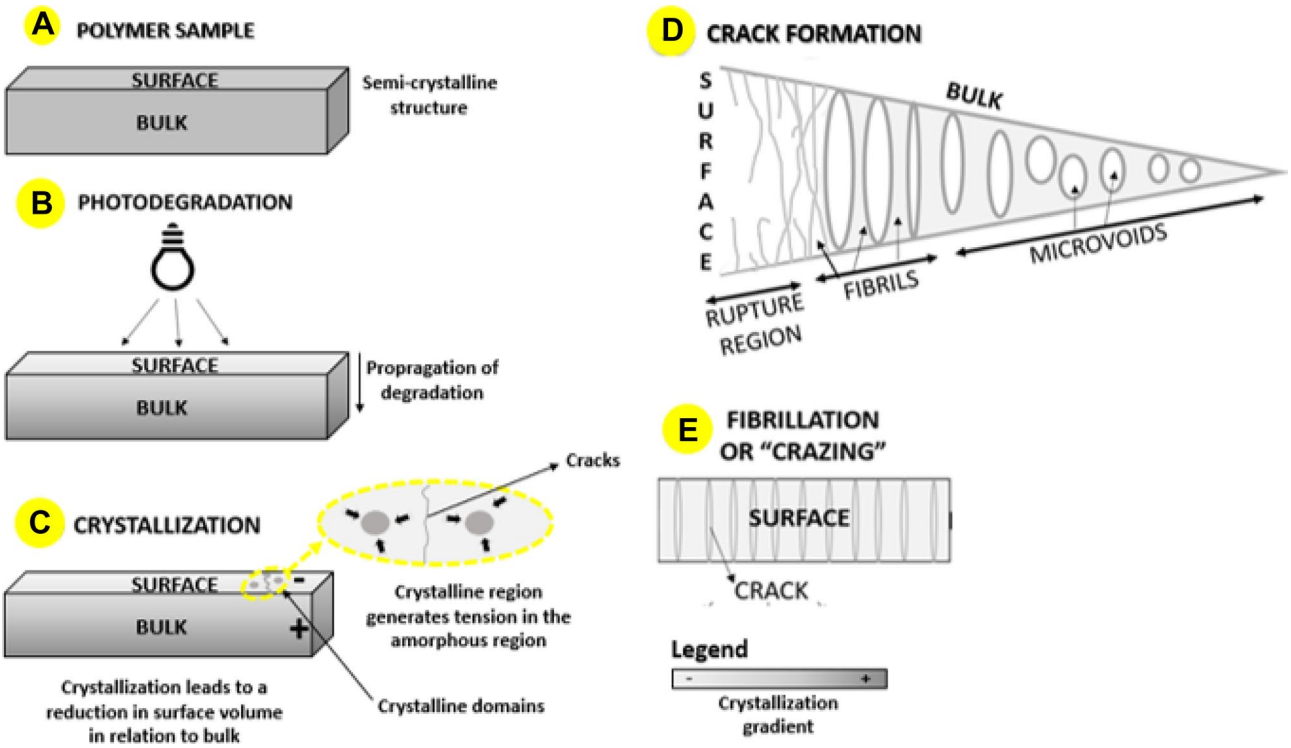

Fig. 6 Schematic representation of the proposed cracking process: **A** Exposure of the polymeric surface to light, leading to gradual photodegradation, from the surface to the bulk; **B** Volumetric reduction on the surface due to the crystallization caused by the photodegradation; **C** Stresses created in the material due to the volume difference form cracks on the surface of the material. **D** Stages of the crack formation process develop microvoids, which grow to form fibrillar bridges, followed by the narrowing and rupture of fibrils leading to cracks; **E** View of the material surface showing the cracks formed

with the presence of elongated structures inside, similar to that observed in the work of Duan and Williams (1998) [21]. These structures are called fibrils, evidenced by yellow arrows, Fig. 4C. Cracking occurs because the volume decreases due to the crystallization. As the photodegradation deepens, cracking also deepens into the bulk. When increasing the magnification of these structures, it is possible to observe that these structures have irregular dimensions, from approximately 14, 16, and 22 nm (Fig. 4D). These structures are called fibrillar bridges [42] and are responsible for structuring the fissure walls. It is possible to observe the structure between the fissure walls generated by these fibrillar bridges (Fig. 5A , B).

Fibrillar bridges are formed with the advancement of degradation toward the bulk due to the tension generated by crystallization resulting from oxidative degradation. As the degradation process evolves, these fibrils stretch, thin, and break [43], as seen in Fig. 4C, D.

Phenomenon schematic representation

In the phenomenon observed in this work, the stress is not caused by an external tensile load, but by an internal tensile load due to crystallinity, resulting in localized stress. The schematic representation of the process is proposed in Fig. 6.

The proposed process occurs with the semicrystalline polypropylene sample (Fig. 6A) when the PP surface is exposed to UV-C light (Fig. 6B). There is a gradual and continuous photodegradation of the surface, advancing to the bulk, demonstrated by the color gradient, from the lightest to darkest, representing the most photodegraded region to the least degraded. As degradation progresses, the volumetric reduction of the surface area compared to the bulk occurs due to crystallization [23], creating tensions in the material due to the volume difference and forming cracks (Fig. 6C) [44]. The process of inner crack formation is exemplified in Fig. 6D, where microvoids develop in the innermost part of the crack. These small voids grow, forming fibrillar bridges [45]. Fibrillar structures act by holding the crack advancement but suffer the action of stresses and narrow until rupture, leading to cracks. These cracks resulting from the fibrillation process are seen on the surface of the polymeric material, Fig. 6E.

Conclusion

We correlated the crack formation process that occurs in the craze phenomenon (under mechanical stimulus) with the crack formation process resulting from the photodegradation. The FTIR, DMTA, and XRD results confirmed the

evolution of the polypropylene photodegradation process, and the visual analysis of the samples revealed the yellowing and deformation of the materials. SEM micrographs revealed the crack formation and propagation process, very similar to the morphology observed in the craze process. The significant difference between the processes is the stimulus to the formation of cracks. The craze phenomenon occurs by an applied stress, such as tensile stress on the material, whereas the cracking, tensile load is caused by walls pulling apart due to photodegradation.

Supplementary Information The online version contains supplementary material available at https://doi.org/10.1007/s10965-022-03357-z.

Acknowledgements This work was financed in part by the Coordination for the Improvement of Higher Education Personnel (CAPES)—Financing Code 001. Process Number: 88882.430936/2019-01 (ASMF), 88882.427090/2019-01 (JSR). São Paulo State Research Support Foundation (FAPESP), projects 2016/24936-3 (WRW), 2019/15976-0 (APL) and 2019/19401-1 (VRB). And National Council for Scientific and Technological Development (CNPq), grant 313989/2018-4 (APL). The authors thank the LNNano/CNPEM – Campinas, Brazil for the SEM analysis.

Author contributions ASMF photodegraded the samples, performed the FTIR and XRD analyses, discussed the results, designed, and drafted the manuscript. JSR performed the dynamic thermal mechanical analysis and contributed to the discussions and drafting of the manuscript. WRW performed the SEM analysis, supervised the work, and contributed to the discussions and the work writing. SAC Contributed to the main conceptual formation of the paper, helping to discuss the results. APL and VRB contributed to the discussions and corrections of the manuscript.

Data availability The raw/processed data required to reproduce these findings cannot be shared at this time due to technical or time limitations.

Declarations

Competing interest The authors declare that they have no known competing financial interests or personal relationships that could have appeared to influence the work reported in this paper.

References

1. El Fawal GF, Abu-Serie MM, Hassan MA, Elnouby MS (2018) Hydroxyethyl cellulose hydrogel for wound dressing: Fabrication, characterization and in vitro evaluation. Int J Biol Macromol 111:649–659. https://doi.org/10.1016/j.ijbiomac.2018.01.040
2. Yousif E, Haddad R (2013) Photodegradation and photostabilization of polymers, especially polystyrene: Review. Springerplus 2:1–32. https://doi.org/10.1186/2193-1801-2-398
3. Curcio MS, Canela MC, Waldman WR (2018) Selective surface modification of TiO2-coated polypropylene by photodegradation. Eur Polym J 101:177–182. https://doi.org/10.1016/j.eurpolymj.2018.01.036
4. Torikai A, Suzuki K, Fueki K (1983) Photodegradation of polypropylene and polypropylene containing pyrene. Polym Photochem 3:379–390. https://doi.org/10.1016/0144-2880(83)90051-9
5. Mena RL, Cacuro TA, Freitas ASM et al (2020) Polymer photodegradation followed by infrared: A tutorial. Rev Virtual Quim 12:959–968. https://doi.org/10.21577/1984-6835.20200077
6. Blais P, Carlsson DJ, Wiles DM (1972) Surface changes during polypropylene photo-oxidation: A study by infrared spectroscopy and electron microscopy. J Polym Sci Part A-1 Polym Chem 10:1077–1092. https://doi.org/10.1002/pol.1972.150100412
7. Gogotov IN, Barazov SK (2014) The effect of ultraviolet light and temperature on the degradation of composite polypropylene. Int Polym Sci Technol 41:55–58. https://doi.org/10.1177/0307174x1404100313
8. Yakimets I, Lai D, Guigon M (2004) Effect of photo-oxidation cracks on behaviour of thick polypropylene samples. Polym Degrad Stab 86:59–67. https://doi.org/10.1016/j.polymdegradstab.2004.01.013
9. Schoolenberg GE, Vink P (1991) Ultra-violet degradation of polypropylene: 1. Degradation profile and thickness of the embrittled surface layer. Polymer (Guildf) 32:432–437. https://doi.org/10.1016/0032-3861(91)90446-P
10. Silva PPDO, Araujo PLB, Lima TBSD, Araujo ES (2022) The influence of environmental stress cracking (ESC) and gamma irradiation on the mechanical properties of polycarbonate: study of synergistic effects. Mater Res. https://doi.org/10.1590/1980-5373-MR-2021-0342
11. Allen NS, McKellar JF (1979) Photo-chemical reactions in commercial poly(oxymethylene). Polym Degrad Stab 1:47–55. https://doi.org/10.1016/0141-3910(79)90024-7
12. Rabello MS, White JR (1997) Crystallization and melting behaviour of photodegraded polypropylene - I. Chemi-crystallization Polymer (Guildf) 38:6379–6387. https://doi.org/10.1016/S0032-3861(97)00213-9
13. Takahashi J, Yamamoto T, Shizawa K (2010) Modeling and simulation for ductile fracture prediction of crystalline polymer based on craze behavior. Int J Mech Sci 52:266–276. https://doi.org/10.1016/j.ijmecsci.2009.09.028
14. Callister WD (2007) Material science and engenireering: An introduction, 7th ed. John Wiley & Sons, Ltd
15. Arzhakova OV, Prishchepa DV, Dolgova AA, Volynskii AL (2019) The effect of preliminary orientation on environmental crazing of high-density polyethylene films. Polymer (Guildf) 170:179–189. https://doi.org/10.1016/j.polymer.2019.03.019
16. Zhang YM, Zhang WG, Fan M, Xiao ZM (2017) On the interaction between a full craze and a near-by circular inclusion in glassy polymers. Eng Fail Anal 79:441–454. https://doi.org/10.1016/j.engfailanal.2017.05.029
17. Basu S, Mahajan DK, Van Der Giessen E (2005) Micromechanics of the growth of a craze fibril in glassy polymers. Polymer (Guildf) 46:7504–7518. https://doi.org/10.1016/j.polymer.2005.05.148
18. Barreto Luna CB, Da Silva DF, Basílio SKT et al (2015) Desenvolvimento de Blendas Poliméricas visando a Tenacificação dos Polímeros: Uma revisão. Semin Ciências Exatas e Tecnológicas 36:67. https://doi.org/10.5433/1679-0375.2015v36n1p67
19. Michler GH, Balt-Calleja FJ (2012) Deformation phenomena and mechanism. In: Michler GH, Balt-Calleja FJ (eds) Nano- and Micromechanics of Polymers: Structure Modification and Improvement of Properties. Hanser Publications, Cincinnati, pp 95–117. https://doi.org/10.3139/9783446428447
20. Beardmore P, Rabinowitz S (1975) Craze formation and growth in anisotropic polymers. J Mater Sci 10:1763–1770. https://doi.org/10.1007/BF00554938
21. Duan DM, Williams JG (1998) Craze testing for tough polyethylene. J Mater Sci 33:625–638. https://doi.org/10.1023/A:1004369107748
22. Øysæd H, Ruyter IE (1987) Formation and growth of crazes in multiphase acrylic systems. J Mater Sci 22:3373–3378. https://doi.org/10.1007/BF01161207

23. Cacuro TA, Freitas ASM, Waldman WR (2018) Demonstration of polymer photodegradation using a simple apparatus. J Chem Educ 95:2222–2226. https://doi.org/10.1021/acs.jchemed.7b00836
24. Masry M, Rossignol S, Gardette JL et al (2021) Characteristics, fate, and impact of marine plastic debris exposed to sunlight: A review. Mar Pollut Bull 171:112701. https://doi.org/10.1016/j.marpolbul.2021.112701
25. Rouillon C, Bussiere PO, Desnoux E et al (2016) Is carbonyl index a quantitative probe to monitor polypropylene photodegradation? Polym Degrad Stab 128:200–208. https://doi.org/10.1016/j.polymdegradstab.2015.12.011
26. Waldman WR, De Paoli MA (2008) Photodegradation of polypropylene/polystyrene blends: Styrene-butadiene-styrene compatibilisation effect. Polym Degrad Stab 93:273–280. https://doi.org/10.1016/j.polymdegradstab.2007.09.003
27. Garcia-Granda S, Montejo-Bernardo JM (2004) X-ray absorption and diffraction - x-ray diffraction - powder. Encycl Anal Sci Second Ed 389–397. https://doi.org/10.1016/B0-12-369397-7/00671-3
28. Craig IH, White JR, Kin PC (2005) Crystallization and chemicrystallization of recycled photo-degraded polypropylene. Polymer (Guildf) 46:505–512. https://doi.org/10.1016/j.polymer.2004.11.019
29. Pae KD, Chu HC, Lee JK, Kim JH (2000) Healing of stress-whitening in polyethylene and polypropylene at or below room temperature. Polym Eng Sci 40:1783–1795. https://doi.org/10.1002/pen.11310
30. Lu Y, Men Y (2018) Cavitation-induced stress whitening in semicrystalline polymers. Macromol Mater Eng 303:1–31. https://doi.org/10.1002/mame.201800203
31. Edge M, Allen NS, Wiles R et al (1995) Identification of luminescent species contributing to the yellowing of poly(ethyleneterephthalate) on degradation. Polymer (Guildf) 36:227–234. https://doi.org/10.1016/0032-3861(95)91308-T
32. Rosu D, Rosu L, Cascaval CN (2009) IR-change and yellowing of polyurethane as a result of UV irradiation. Polym Degrad Stab 94:591–596. https://doi.org/10.1016/j.polymdegradstab.2009.01.013
33. Bangee OD, Wilson VH, East GC, Holme I (1995) Antioxidant-induced yellowing of textiles. Polym Degrad Stab 50:313–317. https://doi.org/10.1016/0141-3910(95)00156-5
34. Sousa AR, Amorim KLE, Medeiros ES et al (2006) The combined effect of photodegradation and stress cracking in polystyrene. Polym Degrad Stab 91:1504–1512. https://doi.org/10.1016/j.polymdegradstab.2005.10.002
35. Antunes MCM, Felisberti MI (2005) Blends of poly(hydroxybutyrate) and poly (ε-caprolactone) obtained from melting mixture. Polimeros 15:134–138. https://doi.org/10.1590/S0104-14282005000200014
36. Psimadas D, Georgoulias P, Valotassiou V, Loudos G (2012) Molecular nanomedicine towards cancer. J Pharm Sci 101:2271–2280. https://doi.org/10.1002/jps.23146
37. Galeski A (2003) Strength and toughness of crystalline polymer systems. Prog Poly Sci 28:1643–1699. https://doi.org/10.1016/j.progpolymsci.2003.09.003
38. Diani J, Gall K (2006) Finite strain 3D thermoviscoelastic constitutive model. Polym Eng Sci 46:86–492. https://doi.org/10.1002/pen
39. Buchasan KJ, McGill WJ (1979) Photodegradation of poly(vinyl esters)—II. Volatile product formation and changes in the absorption spectra and molecular mass distributions. Eur Polym J 16:313–318. https://doi.org/10.1016/0014-3057(80)90075-0
40. Dufresne A (2017) Cellulose nanomaterial reinforced polymer nanocomposites. Curr Opin Colloid Interface Sci 29:1–8. https://doi.org/10.1016/j.cocis.2017.01.004
41. Burmistrov VA, Lipatova IM, Rodicheva JA et al (2019) Rheological, dynamic mechanical and transport properties of compatibilized starch/synthetic copolymer blends. Eur Polym J 120:109209. https://doi.org/10.1016/j.eurpolymj.2019.08.036
42. Motamedian HR, Halilovic AE, Kulachenko A (2019) Mechanisms of strength and stiffness improvement of paper after PFI refining with a focus on the effect of fines. Cellulose 26:4099–4124. https://doi.org/10.1007/s10570-019-02349-5
43. Conway KM, Pataky GJ (2019) Crazing in additively manufactured acrylonitrile butadiene styrene. Eng Fract Mech 211:114–124. https://doi.org/10.1016/j.engfracmech.2019.02.020
44. Argon AS (2011) Craze initiation in glassy polymers - Revisited. Polymer (Guildf) 52:2319–2327. https://doi.org/10.1016/j.polymer.2011.03.019
45. Yarysheva AY, Bagrov DV, Bakirov AV et al (2018) Effect of initial polypropylene structure on its deformation via crazing mechanism in a liquid medium. Eur Polym J 100:233–240. https://doi.org/10.1016/j.eurpolymj.2018.01.040